**The EMBO Journal (2011) 30,** 3701–3713 | © 2011 European Molecular Biology Organization | All Rights Reserved 0261-4189/11
www.embojournal.org

THE EMBO JOURNAL

# A *Drosophila* metallophosphoesterase mediates deglycosylation of rhodopsin

**Jinguo Cao[1,3], Yi Li[1,3], Wenjing Xia[1], Keith Reddig[2], Wen Hu[1], Wei Xie[1], Hong-Sheng Li[2,*] and Junhai Han[1,*]**

[1]Institute of Life Science, The Key Laboratory of Developmental Genes and Human Disease, Southeast University, Nanjing, China and [2]Department of Neurobiology, University of Massachusetts Medical School, Worcester, MA, USA

**Oligosaccharide chains of newly synthesized membrane receptors are trimmed and modified to optimize their trafficking and/or signalling before delivery to the cell surface. For most membrane receptors, the functional significance of oligosaccharide chain modification is unknown. During the maturation of Rh1 rhodopsin, a *Drosophila* light receptor, the oligosaccharide chain is trimmed extensively. Neither the functional significance of this modification nor the enzymes mediating this process are known. Here, we identify a *dmppe* (*Drosophila metallophosphoesterase*) mutant with incomplete deglycosylation of Rh1, and show that the retained oligosaccharide chain does not affect Rh1 localization or signalling. The incomplete deglycosylation, however, renders Rh1 more sensitive to endocytic degradation, and causes morphological and functional defects in photoreceptors of aged *dmppe* flies. We further demonstrate that the dMPPE protein functions as an $Mn^{2+}/Zn^{2+}$-dependent phosphoesterase and mediates *in vivo* dephosphorylation of α-Man-II. Most importantly, the dephosphorylated α-Man-II is required for the removal of the Rh1 oligosaccharide chain. These observations suggest that the glycosylation status of membrane proteins is controlled through phosphorylation/dephosphorylation, and that MPPE acts as the phosphoesterase in this regulation.**

*The EMBO Journal* (2011) **30,** 3701–3713. doi:10.1038/emboj.2011.254; Published online 29 July 2011
*Subject Categories*: membranes & transport
*Keywords*: α-Man-II; deglycosylation; membrane receptor trafficking; metallophosphoesterase; rhodopsin

*Corresponding authors. H-S Li, Department of Neurobiology, University of Massachusetts Medical School, 364 Plantation Street, Worcester, MA 01605, USA. Tel.: +1 508 856 6702; Fax: +1 508 856 6070; E-mail: hong-sheng.li@umassmed.edu or J Han, Institute of Life Science, The Key Laboratory of Developmental Genes and Human Disease, Southeast University, 2 Sipailou Road, Nanjing, Jiangsu 210096, China. Tel.: +86 25 8379 0962; Fax: +86 25 8379 0962; E-mail: junhaihan@seu.edu.cn
[3]These authors contributed equally to this work

**Received: 18 January 2011; accepted: 1 July 2011; published online: 29 July 2011**

## Introduction

N-linked glycosylation within the endoplasmic reticulum (ER) (Kornfeld and Kornfeld, 1985; Helenius, 1994) is important for the folding, assembly, oligomerization, quality control, and subcellular localization of membrane receptors and secretory proteins (Helenius, 1994; Fiedler and Simons, 1995; Helenius and Aebi, 2001). Elimination of glycoprotein N-glycosylation sites frequently results in significantly reduced levels of protein secretion (Fiedler and Simons, 1995). During transportation from ER to the cell surface, the oligosaccharide chains of glycoproteins are trimmed and in many cases are added with new sugar residues. The glycosylation status of membrane proteins is a key determinant for the specificity and efficacy of cell–protein and cell–cell interactions (Varki, 1993; Dwek, 1996). Appropriate N-glycosylation also increases the stability of glycoprotein by increasing plasma residence times (Hoffmeister *et al*, 2003) and providing steric protection from proteases and non-specific interactions (Rudd *et al*, 2001).

In photoreceptor neurons, N-glycosylation of the light receptor rhodopsin is critical for its exit from the ER and for its targeting to light sensory organelles (Hargrave, 1977). Pharmacologically blocking rhodopsin glycosylation has prevented newly synthesized rhodopsin from maturation and inhibited the membrane disc morphogenesis (Fliesler *et al*, 1984, 1986). Importantly, mutations at the sites of N-glycosylation in rhodopsin have been identified in patients of autosomal dominant retinitis pigmentosa (Dryja and Li, 1995; Papermaster, 1995), a retinal degeneration disorder that causes visual defects including night blindness and tunnel vision (Dryja and Li, 1995).

Rh1, the major rhodopsin in *Drosophila*, undergoes N-glycosylation during biosynthesis (O'Tousa, 1992; Brown *et al*, 1994). Mutation of residue $asn^{20}$, the single site of N-glycosylation in Rh1, retains Rh1 in the secretary pathway and drastically reduces the level of mature Rh1 (Webel *et al*, 2000). Interestingly, the oligosaccharide chain is either extensively trimmed or completely removed in mature Rh1 (Huber *et al*, 1990; Katanosaka *et al*, 1998), indicating that Rh1 undergoes deglycosylation during its transport from ER to the light sensory organelle rhabdomere (Satoh *et al*, 1997). However, the enzymes mediating this process remain unknown. More importantly, the physiological significance of the Rh1 deglycosylation is unclear.

Metallophosphoesterases (MPPEs) are a superfamily of enzymes that contain two well-characterized groups, phosphomonoesterases and phosphodiesterases. The activity of MPPEs depends on the presence of metal ions such as $Mn^{2+}$, $Ni^{2+}$, $Mg^{2+}$, $Zn^{2+}$, $Fe^{2+}$ and $Co^{2+}$ (Cohen, 1989). A wide variety of proteins and nucleotides are MPPE substrates, including protein phosphoserine phosphatases, sphingomyelin phosphodiesterases, nucleotidases, 2′,3′-cAMP phosphodiesterases and nucleases (Aravind and Koonin, 1998; Keppetipola and Shuman, 2008; Fujita *et al*, 2009). A recent

study suggested that PGAP5, a human MPPE, mediated the remodelling of the glycan moiety on glycosylphosphatidylinositol-anchored proteins by removal of a side-chain ethanolamine-phosphate from the second mannose of glycosylphosphatidylinositol (Fujita *et al*, 2009). Although several MPPEs have been characterized based on their biochemical activity and structure, their native substrates are largely unknown. More importantly, *in vivo* functions of these enzymes have yet to be well characterized (Chen *et al*, 2004).

CG8889, the *Drosophila* orthologue of human metallophosphoesterase 1, is highly expressed in the eye (Xu *et al*, 2004). In this work, we demonstrate that CG8889, hereafter referred to as dMPPE, functions as a phosphoesterase, and is required for Rh1 deglycosylation in photoreceptor neurons. Our study presents the first evidence that the glycosylation status of membrane receptors can be regulated through phosphorylation/dephosphorylation.

## Results

### *Rh1 has a higher molecular weight in a dmppe mutant*

We obtained a *dmppe* mutant, $CG8889^{e02905}$, from the Harvard Exelixis Collection. In newly eclosed, dark-reared mutants, we detected a small reduction in light sensitivity of the fly eye based on electroretinogram (ERG) recordings (Figure 1A and B). As light sensitivity is largely determined by the density of rhodopsin in the rhabdomeral membrane (Johnson and Pak, 1986), we stained cross-sections of eye with an Rh1 antibody to examine the Rh1 level in rhabdomeres. In this experiment, flies were reared in the dark from early pupal stage to prevent light-induced endocytosis. Four hours after eclosion, the majority of Rh1 protein was localized in the rhabdomere in wild-type flies. In contrast, in the *dmppe* mutant, many Rh1-positive vesicles (RPVs) were detected in the cell body of photoreceptors (Figure 1C). It is previously reported that Rh1 transports to rhabdomere through multivesicular bodies (MVBs; Satoh *et al*, 2005). To investigate whether the RPVs in the mutant were MVBs, we stained eye sections with the Rh1 and an immunogold antibody, and examined the result via electron microscopy (EM). The EM images revealed that RPVs appeared to be collections of small vesicles (Figure 1D), which are reminiscent of the reported MVBs. Thus, Rh1 could be retained in the secretion pathway in the mutant.

We further compared the Rh1 protein level between wild type and the mutant using western blots. The results showed a slight reduction of Rh1 level in the newly eclosed mutant and normal Rh1 protein levels in 1-day-old mutants (Figure 1E). Intriguingly, in the mutant, we observed an increase in the molecular weight (MW) of Rh1 (Figure 1E and F), while all other visual molecules examined were similar to wild type (Figure 1F). The mRNA sequence of *ninaE*, the gene encoding the Rh1 protein, was not changed in the mutant (data not shown); therefore, the increase in Rh1 MW is due to abnormal post-translational modification.

### *The increase in Rh1 MW is due to a failure of deglycosylation*

As dMPPE is predicted to be a phosphoesterase, the increase in Rh1 MW could be due to hyperphosphorylation. However, the following observations argue against this explanation. First, treatments with non-specific phosphatases, calf intestinal phosphatase or potato acid phosphatase, did not change the MW of Rh1 purified from the mutant (Figure 2A). Second, a truncated Rh1 protein encoded by the mutant allele $ninaE^{\Delta 365}$, which lacks the phosphorylation sites (Vinos *et al*, 1997), still had an increased MW in the *dmppe* mutant background (Figure 2B).

As the MW of Rh1 from the mutant is close to that of immature and glycosylated Rh1, we purified Rh1 proteins from both wild type and mutant using Rh1 antibody-linked affinity beads and treated them with different glycosidases. After treatment with peptide: N-glycosidase F (PNGase F), the MW of Rh1 from the mutant was reduced (Figure 2C), indicating that Rh1 is glycosylated in the mutant. As a control, the mature Rh1 protein from wild type showed undetectable change in the MW (Figure 2C).

To characterize the oligosaccharide chain present on glycosylated Rh1, we digested Rh1 from the mutant with endoglycosidase H (Endo H). Endo H only cleaves unmodified core oligosaccharides but not complex N-linked glycoproteins (Twining, 1984). The result showed that Rh1 from the mutant was deglycosylated by Endo H (Figure 2D), suggesting that Rh1 in the mutant contains a core oligosaccharide.

### *Rh1 transport is slow in the dmppe mutant*

To understand why some Rh1 protein mislocalized in the newly eclosed mutant, we examined the dynamics of Rh1 glycosylation and distribution in both wild type and the mutant. Western blots of wild type showed that Rh1 was undetectable at 63% of pupal development (% pd), while immature 40 kDa Rh1 was detected at 68% pd, and mature 36 kDa Rh1 was detected at 71% pd (Figure 3A). Thus, the extensively trimmed Rh1 begins to form between 68% and 71% pd. In immunostaining experiments, most Rh1 protein resides in the cell body but not in the rhabdomere at 68% pd, ~25% of Rh1 resides in the rhabdomere at 71% pd and ~86% of Rh1 resides in the rhabdomere at 79% pd (Figure 3C and E). Taken together, these observations suggest that the immature high-MW Rh1 mostly exists in the cell body and the mature low-MW form localizes in the rhabdomere. In other words, Rh1 undergoes oligosaccharide trimming during its trafficking to the rhabdomere.

In contrast, in the *dmppe* mutant, at ~68% pd, the Rh1 MW was 40 kDa. It changed gradually to 39 kDa during development and remained the same size through eclosion (Figure 3B). These observations suggest that the process of Rh1 deglycosylation is disrupted in the mutant. Unlike the wild type, the mutant showed almost no Rh1 in the rhabdomere before 71% pd, and only ~49% of Rh1 was localized in the rhabdomere at 79% pd (Figure 3D and E). These data indicate that oligosaccharide trimming accelerates the transport of Rh1 to the rhabdomere.

Although we detected some RPVs in the cytoplasm, most of the glycosylated Rh1 was still loaded into rhabdomere in the newly eclosed mutant. To investigate the fate of RPVs, we examined the distribution and protein level of Rh1 in more matured adults. In 2-day-old, dark-reared mutants, Rh1 was completely localized in the rhabdomere (Figure 3F), and the overall Rh1 level was comparable to wild type (Figure 3G), suggesting that Rh1 in the RPVs ultimately transfers to the rhabdomere.

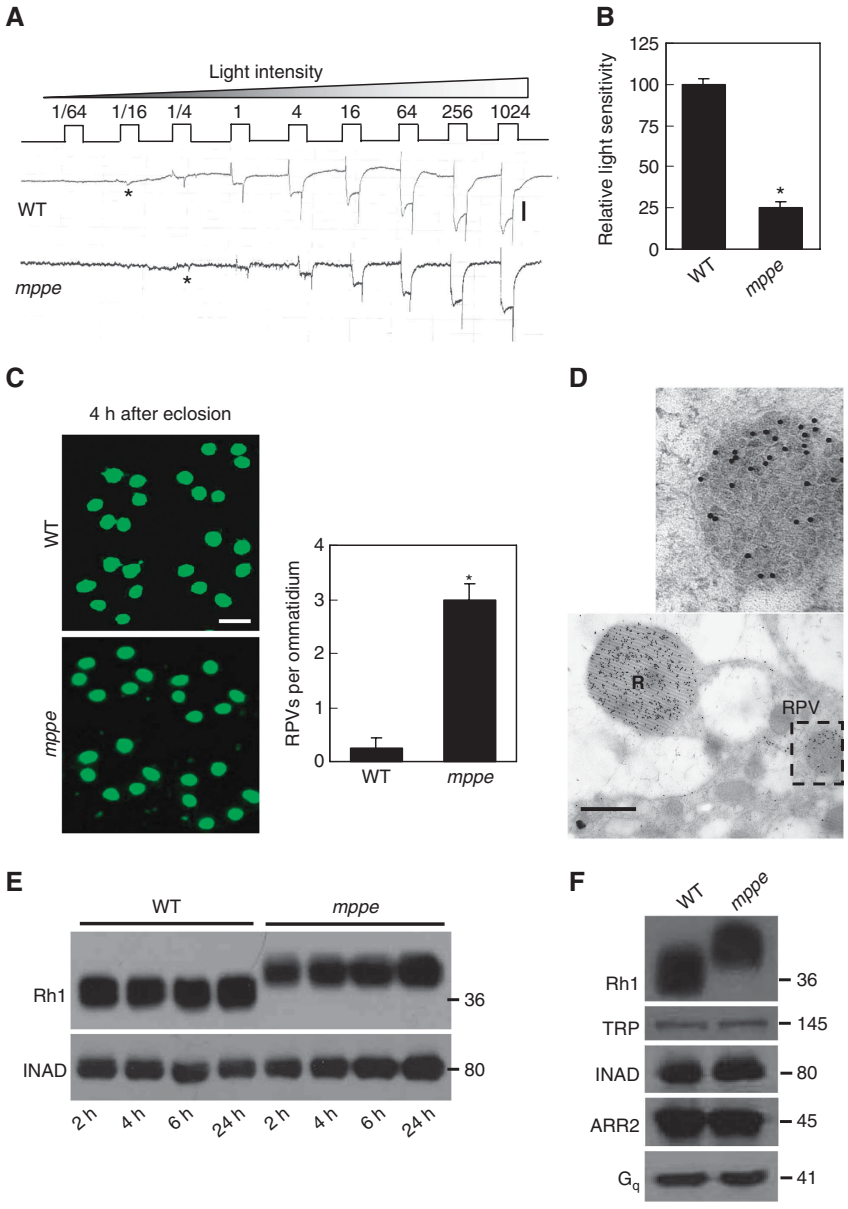


**Figure 1** Newly eclosed *dmppe* mutants show reduced light sensitivity, abnormal distribution and high molecular weight of Rh1. (**A**) ERG recordings revealed the reduction of light sensitivity in newly eclosed *dmppe* mutants. Flies were raised in the dark and examined within 4 h after eclosion. Fly eyes were stimulated with a series of 1 s light pulses of increasing intensities as labelled on the top. The first response appearing is marked with an asterisk. The scale bar next to the top trace is 5 mV. (**B**) Quantification of light sensitivities in newly eclosed flies. The mean relative sensitivities shown were calculated as described in Materials and methods. The error bar represents standard error of the mean (s.e.m.). *Indicates that the sample is significantly different from others in the group. (**C**) Rh1 distribution in the photoreceptors of newly eclosed flies. Cross-sections were prepared as described in Materials and methods. The sections were stained with a monoclonal Rh1 antibody (4C5). The number of RPVs per ommatidium was calculated for each genotype. Scale bar, 5 μm. (**D**) Immunogold electron microscopy reveals that RPV appeared to be the aggregation of small vesicles. Sections were prepared as described in Materials and methods. One RPV (boxed) is enlarged in the upper panel. Scale bar, 2 μm. (**E**) Reduction of Rh1 level in newly eclosed *dmppe* mutants. Flies were raised in the dark and heads were collected at the indicated time after eclosion. The scaffold protein INAD was probed in parallel. (**F**) Western blots show the increase in Rh1 MW in the mutant. The MWs of other visual molecules are normal. WT: wild type.

### *Deglycosylation is not required for the normal signalling of Rh1*

Glycosylated Rh1 localized normally in the rhabdomere in matured mutants and the rhabdomeral density of Rh1 was comparable to wild type; therefore, we next examined whether the retained oligosaccharide chain interfered with the signalling of Rh1. Compared with the wild-type flies, 2-day-old, dark-reared mutants displayed normal ERG recording traces (Supplementary Figure S1A), ERG amplitude (Supplementary Figure S1B), ON and OFF transients (Supplementary Figure S1C) and sensitivity to light (Supplementary Figure S1D). These data indicate that the deglycosylation of Rh1 is not required for the normal activation of visual signalling.

In addition, the deglycosylation of Rh1 was also not required for the normal deactivation of visual signalling. In 2-day-old, dark-reared mutants, the termination speed of light response and the minimum light intensity required to

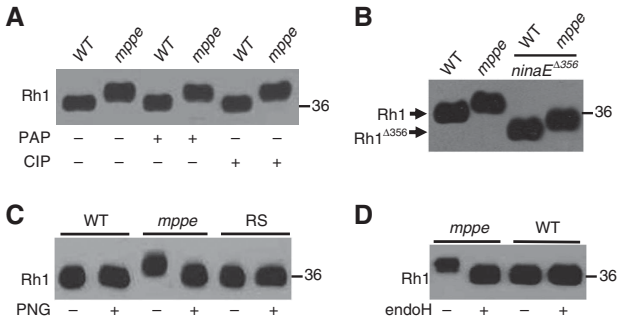


**Figure 2** The increase in Rh1 MW is due to a failure of deglycosylation. (**A**) The increase in Rh1 MW is not caused by phosphorylation modification. After digestion with calf intestinal phosphatase (CIP) or potato acid phosphatase (PAP) at 37°C for 16 h, purified Rh1 was subjected to SDS–PAGE and then immunoblotting. (**B**) Deletion of phosphorylation sites in Rh1 did not prevent the increase in Rh1 MW in the mutant background. Each lane was loaded with one fly head and probed with a polyclonal antibody against the N terminus of Rh1. Note: in the $ninaE^{\Delta 356}$ allele, only truncated Rh1 can be detected, as this mutant allele was crossed into a *ninaE* null mutant background. (**C**) Rh1 bands shifted after the treatment with PNGase F. After digestion with PNGase F in 37°C for 16 h, purified Rh1 was subjected to SDS–PAGE and immunoblotting. RS: rescuing flies, *dmppe; p[trp::dmppe]*. +: Incubation with PNGase F. −: Incubation without PNGase F. (**D**) The MW of Rh1 was reduced after the treatment with Endoglycosidase H. Purified Rh1 was incubated with Endoglycosidase H at 37°C for 16 h and examined by western blots.

produce prolonged depolarization after potential were comparable to that of wild type (Supplementary Figure S1E and F).

### *Deglycosylation is essential for the stability of endocytosed Rh1*

Although the deglycosylation of Rh1 is not required for normal visual signalling, old mutants reared in regular light conditions displayed obvious reduced sensitivity to light. ERG recording revealed that the overall light sensitivity of photoreceptor cells strikingly decreased in 20-day-old mutants raised under regular light cycles (12 h light/12 h dark; Figure 4A). Western blotting showed that most Rh1 and much of INAD had been degraded in mutant, but not in wild-type flies (Figure 4B), suggesting that old mutants undergo retinal degeneration. Subsequent EM examinations revealed many small splits and tiny holes in the rhabdomere of 18-day-old mutants raised in the same condition (Figure 4C). However, 16-day-old, dark-reared mutant displayed normal rhabodomeral structure, Rh1 level, and sensitivity to light (Supplementary Figure S2). Thus, the visual functional defects and retinal degeneration could be due to loss of Rh1 protein. Indeed, retinal degeneration also occurs in *ninaE* mutant flies that have extremely low levels of Rh1 (Leonard *et al*, 1992).

Given that the glycosylation status affects the endocytosis of several membrane receptors (Partridge *et al*, 2004), the reduction of Rh1 in old mutants could be due to excessive endocytosis and subsequent degradation. To test this hypothesis, we first investigated the light-induced Rh1 endocytosis in the mutant. After exposure to regular light (700 lux) for 8 h, the number of endocytic Rh1 particles per ommatidium in the mutant was comparable to that in wild type (2.3 ± 0.3 versus 2.6 ± 0.4; Figure 4D). This observation suggests that the oligosaccharide chain does not significantly interfere with Rh1 endocytosis.

Since glycosylation of Rh1 does not affect its endocytosis, we next examined whether glycosylation of Rh1 changed the stability of endocytosed Rh1. For this purpose, we prevented the endocytosed Rh1 from being recycled back to the rhabdomere by stimulating the fly with pure blue light, which converts the inactive Rh1 rhodopsin to the active metarhodopsin, but does not change it back to rhodopsin for recycling (Xu *et al*, 2004; Han *et al*, 2007). After 2 h of blue light stimulation (700 lux), equal ratios of endocytosed Rh1 signal were detected in wild type and the mutant (4.8 ± 0.5 versus 5.1 ± 0.6%; Figure 4E). At this time point, the degradation of endocytosed Rh1 had not begun in either fly (Figure 4F). After 3 h of stimulation, however, significant Rh1 degradation was observed in the *dmppe* mutant (Figure 4F). In addition, the intensity of visible endocytic Rh1 signal increased further only in the wild type (arrows in Figure 4E) but not in the mutant (Figure 4E). Thus, the insufficiently deglycosylated Rh1, after endocytosis, is not as stable as the extensively processed Rh1.

### *dMPPE mediates the process of Rh1 deglycosylation*

In the *dmppe* mutant, a p element is inserted into the 5′ untranslated region of the *dmppe* gene. Homozygotes of this allele are viable. To determine if this insertion actually disrupts the *dmppe* gene, we examined *dmppe* mRNA levels with northern blot analysis and real-time RT–PCR. Using a probe that specifically recognizes a long transcriptional form of *dmppe* mRNA, we confirmed the loss of *dmppe* mRNA in the mutant (Figure 5A). Using real-time RT–PCR, we showed that the amount of *dmppe* mRNA decreased ∼50-fold in the mutant (Figure 5B). Furthermore, western blots also demonstrated the absence of dMPPE protein in the mutant (Figure 5C). Thus, the *dmppe* gene is disrupted by this p element insertion.

To confirm that loss of dMPPE is responsible for the defect in Rh1 deglycosylation, we attempted to rescue the phenotype by generating transgenic flies that express a dMPPE cDNA. In a *cn,dmppe,bw; p[hs-dmppe]* fly, expression of dMPPE from the pupal stage converted Rh1 to the extensively processed form (Figure 5D). To show that dMPPE functions in the photoreceptor, we successfully rescued the defect of Rh1 deglycosylation in another transgenic fly (*cn, dmppe,bw; p[trp::dmppe]*) that expresses dMPPE through a photoreceptor-specific *trp* gene promoter (Han *et al*, 2006; Figure 5E). In this latter fly, we also observed the rescue of two other phenotypes of the *dmppe* mutant: the incomplete Rh1 delivery (Figure 5F) and the reduction of light sensitivity (Figure 5G) in newly eclosed flies. Taken together, the above observations indicate that dMPPE is required for the deglycosylation of Rh1.

### *dMPPE predominately localizes in Golgi and colocalizes with trafficking Rh1*

To investigate why dMPPE is required for Rh1 deglycosylation, we first examined the expression pattern of dMPPE in the adult fly head, and determined that dMPPE was highly expressed in the retina (Figure 6A). We next stained the dissected ommatidium with both anti-Rh1 and anti-dMPPE antibodies to display the subcellular localization of dMPPE.

 

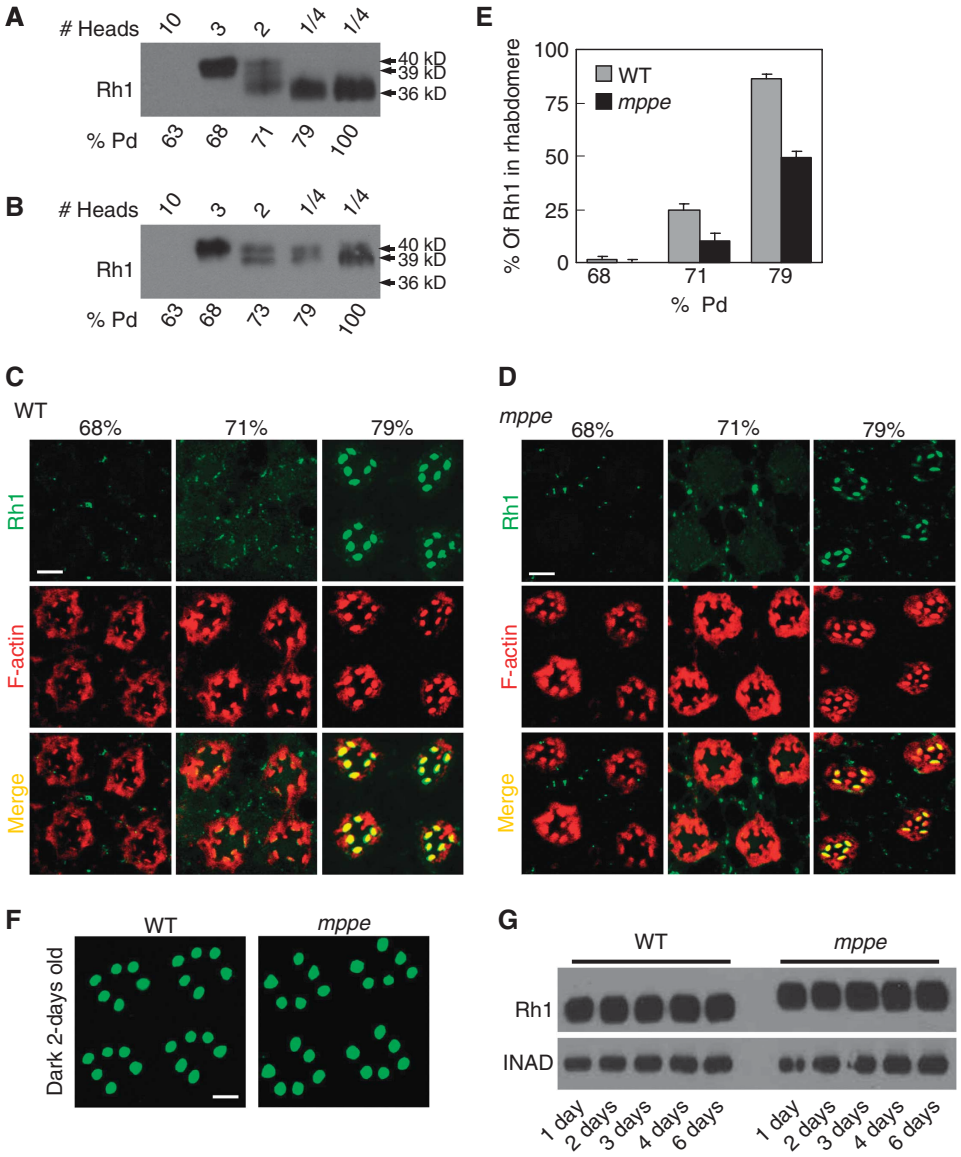


**Figure 3** Deglycosylation of Rh1 is essential for transport, but not required for membrane localization. (**A**) Time course of Rh1 processing in wild-type flies. Pupal heads were collected at the indicated time. The amount loaded is labelled on the top. (**B**) The Rh1 deglycosylation process is disrupted in *dmppe* mutant. Pupae were collected at different pupal development time points. (**C**) Rh1 distribution in the developing photoreceptors of wild-type flies. Sections were prepared as described in Materials and methods. Cross-sections were stained with anti-Rh1 antibody (green) and rhodamine-phalloidin (red). % pd: % of pupal development. Scale bar, 5 μm. (**D**) Rh1 distribution in the developing photoreceptors of the *dmppe* mutant. Scale bar, 5 μm. (**E**) Quantification of the percentage of Rh1 in rhabdomere during pupal development. Quantification was performed as described in Materials and methods. (**F**) Most Rh1 localized normally in matured mutant photoreceptors. Flies were raised in the dark and examined at 2 days after eclosion. Collection and fixation were performed under dim red light. Scale bar, 5 μm. (**G**) Constant Rh1 levels in adult mutants. Flies were raised in the dark and examined at the indicated time after eclosion. The scaffold protein INAD was probed in parallel as a loading control.

The images showed that dMPPE resides in the cell body of photoreceptors, with some surrounding the nucleus (Figure 6B). To further display the organellar distribution of endogenous dMPPE, we stained dissected ommatidium, whose ER or Golgi had been labelled with GFP. The results showed that dMPPE predominately exists in the Golgi (Figure 6C and D).

Since dMPPE mediates the process of Rh1 deglycosylation, we next examined the distribution of dMPPE during Rh1 maturation. At 68% pd, dMPPE partially colocalized with Rh1 (Figure 6E), suggesting dMPPE mediates Rh1 deglycosylation during immature Rh1 trafficking.

### *dMPPE functions as a phosphoesterase and its phosphoesterase activity is essential for Rh1 deglycosylation*

To test whether dMPPE can directly remove the oligosaccharide chain from glycosylated Rh1, we treated the glycosylated Rh1 from the mutant with purified recombinant dMPPE. After 16 h of incubation, the Rh1 band showed no size shift (Supplementary Figure S3). Thus, dMPPE cannot directly remove the oligosaccharide chain from Rh1.

Instead, dMPPE functions as a phosphoesterase, as predicted, supported by the following observations. First, in *p[hs::dmppe]* transgenic flies, the total phosphoesterase

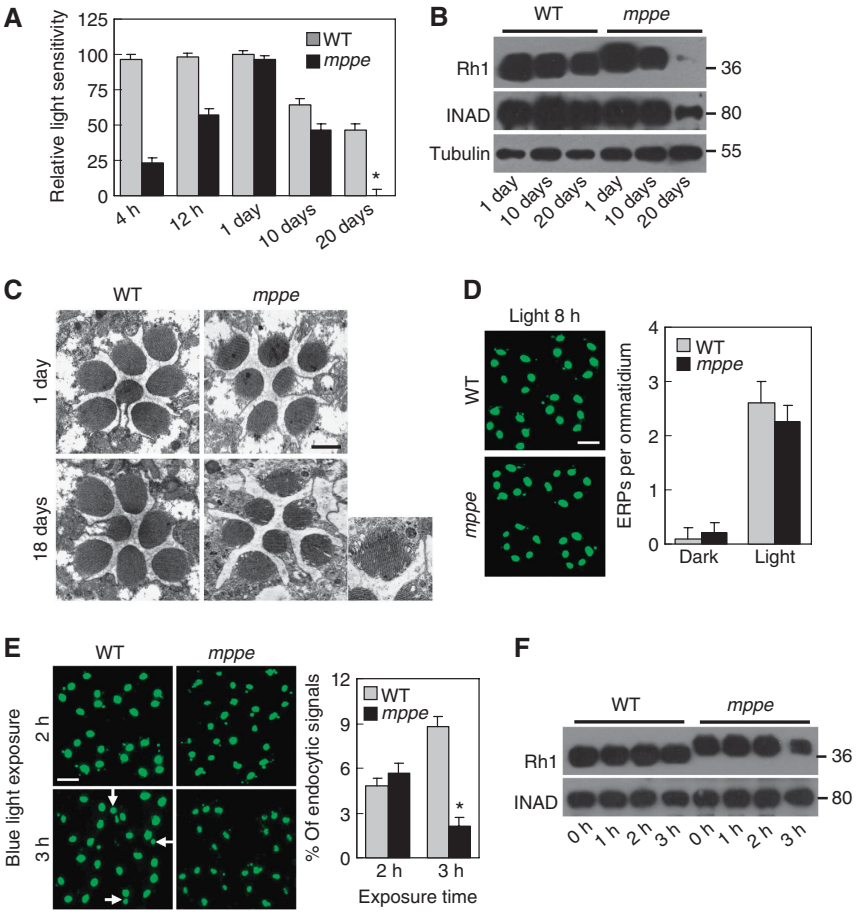


**Figure 4** Glycosylated Rh1 is not stable once it is endocytosed, and leads to retinal degeneration. (**A**) Quantification of light sensitivities in wild-type and *dmppe* mutant flies. Flies were raised in 12 h light/12 h dark conditions. Newly eclosed adults were collected and reared for the indicated time. For 1-day-old flies, collected adults were reared for 24 h. Relative light sensitivity was measured and calculated as described in Materials and methods. (**B**) Rh1 and INAD levels decreased in the older mutant. Tubulin was probed as a loading control. The reduction of INAD level indicates the older mutant undergoes retinal degeneration. (**C**) EM analyses revealed the older mutant underwent retinal degeneration. Flies were raised in 12 h light/12 h dark conditions for the indicated time. Each picture shows a single ommatidium. One degenerated rhabdomere from the mutant is enlarged in the right panel. Scale bar, 2 μm. (**D**) Glycosylation does not affect light-induced endocytosis of Rh1. Two-day-old dark-reared flies were stimulated with white light (700 lux) for 8 h and stained with the monoclonal Rh1 antibody. Scale bar, 5 μm. (**E**) Rh1 distribution after blue light stimulation. Two-day-old, dark-reared flies were stimulated with pure blue light (700 lux) for 2 or 3 h. Cross-sections were prepared and stained as described in Materials and methods. Three large endocytic Rh1 particles in the cell bodies are marked with arrows. Scale bar, 5 μm. The right panel shows the ratio of Rh1 signal intensity in the cell body for each genotype and treatment. Quantification was performed as described in Materials and methods. (**F**) Rh1 level decreased in the mutant after 3 h under blue light stimulation. Two-day-old, dark-reared flies were stimulated with pure blue light (700 lux) for the indicated time. After stimulation, fly heads were collected and total Rh1 levels were compared by western blots. INAD was probed as a loading control. *indicates that the sample is significantly different from the control ($P<0.01$; Student's *t*-test).

activity of head extract increased gradually from 1 h of heat shock and reached the highest level by 3 h, showing perfect correlation with the increase in dMPPE protein level (Figure 7A). Second, dMPPE proteins purified from transformed bacteria showed remarkable, metal-dependent phosphoesterase activities in the presence of $Mn^{2+}$ or $Zn^{2+}$. Other metal ions, such as $Ca^{2+}$ and $Mg^{2+}$, did not significantly support the phosphoesterase activity of dMPPE (Figure 7B). Finally, once we deleted amino acids 164–183 of dMPPE (dMPPE$^{\Delta}$), the phosphoesterase activity was abolished (Figure 7C).

To determine whether the phosphoesterase activity of dMPPE is required for Rh1 deglycosylation, we generated a transgenic fly that expressed the truncated dMPPE$^{\Delta}$ protein. We failed to rescue the Rh1 deglycosylation defect in this transgenic fly (*cn,dmppe,bw; GMR-Gal4/p[UAS::dmppe$^{\Delta}$]*; Figure 7D), indicating that the phosphoesterase activity of dMPPE is essential for Rh1 deglycosylation.

### *dMPPE dephosphorylates α-Man-II*

It is likely that dMPPE stimulates a glycosidase through dephosphorylation, which in turn catalyses the Rh1 deglycosylation. To test whether dMPPE dephosphorylates any protein *in vivo*, we conducted western blotting experiments with antibodies that recognize phosphorylated proteins, and found that several phosphorylation bands had increased levels in the *dmppe* mutant (Supplementary Figure S4). To identify these proteins, we enriched phosphorylated proteins from both wild-type and mutant flies. After PAGE-gel fractionation, we collected those protein bands that showed increased levels in the mutant background. Using mass spectrometry, we successfully identified two proteins: a glycosidase

 

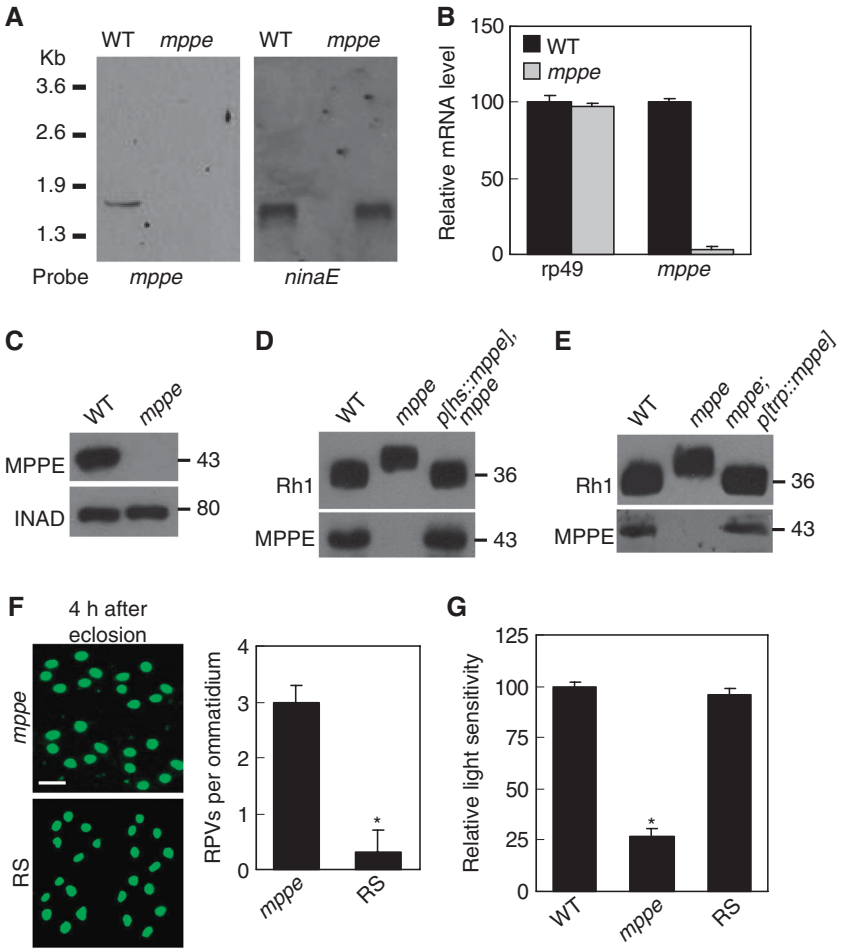


**Figure 5** dMPPE is required for Rh1 deglycosylation. (**A**) Northern blot shows the mRNA of the *dmppe* gene is absent in *dmppe* mutants. Total RNA was isolated from the heads of <3-day-old *cn,bw* and *cn,pBacCG8889*$^{e02905}$*,bw* flies using Trizol. Total RNA (10 μg) was subjected to 1% denaturing agarose gels and hydrated with a DIG-labelled *dmppe* cDNA probe. The membrane was stripped and re-probed with *ninaE* probe for the loading control. (**B**) Real-time RT–PCR reveals that the *dmppe* mRNA level decreases ~50-fold in *dmppe* mutants. Three data sets were averaged. (**C**) Western blots showing loss of dMPPE protein in the mutant. Each lane was loaded with three fly heads. (**D**) Overexpression of dMPPE restored the MW of Rh1. *cn, mppe,bw;p[hs*::*mppe]* flies were heat shocked every day for 1 h from early pupal stage. Newly eclosed adults were collected for western blots. dMPPE protein levels are showed on the lower panel. (**E**) Photoreceptor-specific expression of dMPPE restored the MW of Rh1. dMPPE was specifically expressed in the photoreceptor through a *trp* gene promoter. dMPPE protein levels are shown on the lower panel. (**F**) Rh1 distribution in newly eclosed rescue (RS) flies. Quantifications of RPV number per ommatidium are presented in the right panel. The RS represents *cn, mppe,bw; p[trp*::*mppe]/TM6c* flies. Scale bar, 5 μm. (**G**) Light sensitivity was restored in the RS fly. The relative sensitivities were calculated as described in Materials and methods. *indicates that the sample is significantly different from the control ($P<0.01$; Student's *t*-test).

α-Man-II (Harpaz and Schachter, 1980) and a cuticle protein CG4784 (Figure 8A; Supplementary Table 1). These two proteins are potential substrates of dMPPE.

Considering that α-Man-II could be a glycosidase involved in the Rh1 deglycosylation, we focused on this protein and further identified its phosphorylation sites. First, we generated a myc-tagged α-Man-II transgene and introduced it into both wild-type and *dmmpe* mutant backgrounds (Figure 8B). After immunoprecipitation from fly extracts and digestion with trypsin, the peptides of the myc-tagged α-Man-II were spotted for mass spectrometric analysis. Analysis of the mass spectra revealed a singly charged peptide $[M+H]^+$ ion signal at *m/z* 1901.94 in the mutant sample (Figure 8C) that was not present in the wild-type sample, accompanied by the appearance of a new peptide $[M+H]^+$ ion signal at *m/z* 1821.97, corresponding to the predicted 80 D lost of a phosphate group (Figure 8C). Next, we isolated the phosphorylated peptides of α-Man-II from the digested mutant sample using PHOS-select iron affinity gel. Tandem MS/MS analysis identified the *m/z* 1901.94 ion as residues 69–84 containing a phosphorylation at serine 73 (Supplementary Figure S5).

To test whether dMPPE directly dephosphorylates α-Man-II, we first investigated whether they have overlapping distributions in the cell. In co-transfected HEK 293 cells, immunostaining signals of α-Man-II overlapped with those of dMPPE (Supplementary Figure S6A). Importantly, these two proteins even associated with each other in immunoprecipitation experiments (Supplementary Figure S6B). Next, we conducted *in vitro* dephosphorylation assays on a recombinant α-Man-II protein. After incubation with *dmppe* mutant fly extract, the α-Man-II protein underwent phosphorylation (Figure 8D). This phosphorylation was reversed by subsequent incubation with a purified recombinant dMPPE protein, but not by the truncated dMPPE$^{\Delta}$ protein (Figure 8D). Thus, dMPPE may directly dephosphorylate α-Man-II.

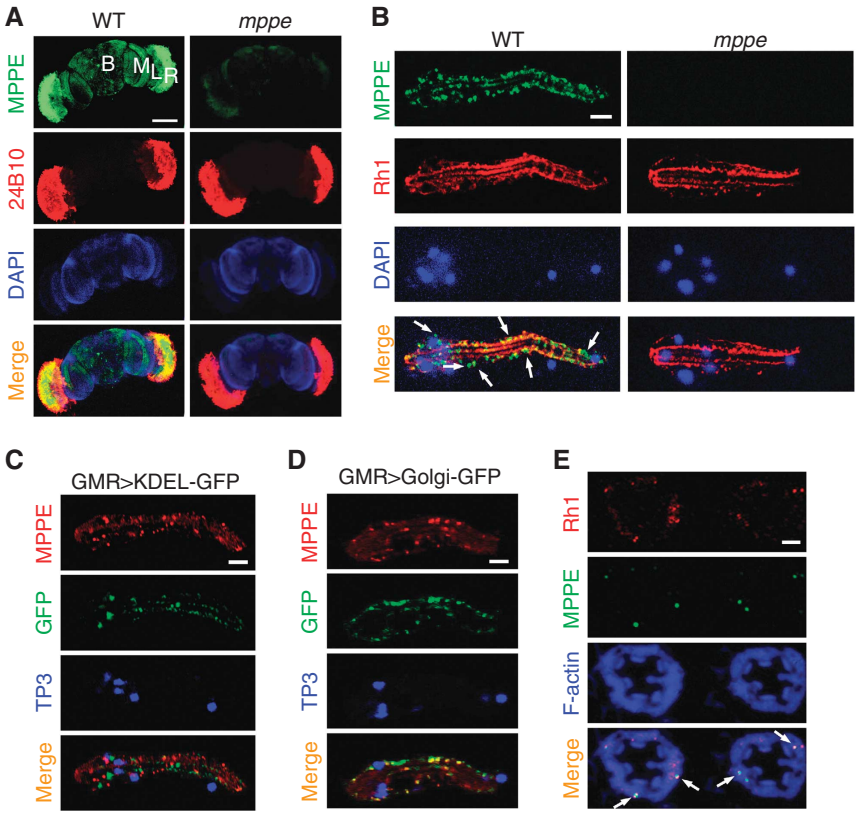


**Figure 6** dMPPE localizes in Golgi and colocalizes with trafficking Rh1. (**A**) dMPPE is predominately expressed in the retina. Dissected fly heads were costained with dMPPE antibody (green), a 24b10 antibody (red, showing retina) and DAPI (blue, for nuclei). R = retina, L = lamina, M = medulla, B = brain. Scale bar, 200 μm. (**B**) dMPPE distribution in photoreceptors. Dissected ommatidia were costained with dMPPE antibody (green), an Rh1 antibody (red, showing rhabdomere bundles) and DAPI (blue, for nuclei). Scale bar, 10 μm. (**C**) In GMR-Gal4/p[UAS::GFP-KDEL] flies, dMPPE does not colocalize with GFP-KEDL. Dissected ommatidia were costained with dMPPE antibody (red), GFP antibody (green, showing ER) and TO-PRO-3 iodide (blue, for nuclei). Scale bar, 10 μm. (**D**) In GMR-Gal4/p[UAS::galactosyltransferase-GFP] flies, dMPPE colocalizes with the GFP signal. Dissected ommatidia were costained with dMPPE antibody (red), GFP antibody (green, showing Golgi) and TO-PRO-3 iodide (blue, for nuclei). Scale bar, 10 μm. (**E**) dMPPE colocalizes with trafficking Rh1 vesicles (arrows). At 68% pd, pupae of wild-type flies were collected. Sections were costained with Rh1 antibody (red), dMPPE antibody (green) and phalloidin (blue, showing rhabdomere bundles). Scale bar, 5 μm.

### *α-Man-II mediates Rh1 deglycosylation in vivo*

It is known that α-Man-II specifically catalyses the removal of both α1,3-linked and α1,6-linked mannoses from GnMan5Gn2 to yield GnMan3Gn2 (Gn, N-acetylglucosamine) (Harpaz and Schachter, 1980; Figure 9F). If the activity of α-Man-II is impaired in the *dmppe* mutant, Rh1 proteins from the mutant would contain a GnMan5Gn2 chain. To test this, we conducted glycosidase digestions to analyse the retained oligosaccharide chain of Rh1 in the mutant. The digestion of α1-6 mannosidase significantly decreased the MW of the mutant Rh1 protein (Figure 9A). However, the digestion of α1-2,3 mannosidase decreased the Rh1 MW even more (Figure 9A). These results suggest that the Rh1 oligosaccharide chain in the *dmppe* mutant contains an unbranched α1, 6-linked mannose and at least two α1-2,3-linked mannoses, consistent with the structure of GnMan5Gn2.

Next, we demonstrated that α-Man-II mediated Rh1 deglycosylation both *in vitro* and *in vivo*. First, purified recombinant α-Man-II protein decreased the MW of Rh1 protein isolated from the *dmppe* mutant (Figure 9B). Second, we generated flies that contain homozygous *α-Man-II* mutant photoreceptors (see Supplementary data), and found that the MW of Rh1 from these flies was the same as in the *dmppe* mutant (Figure 9C). The MW of Rh1 from the *α-Man-II* mutant returned to the wild-type size after PNGase F digestion, indicating a defect in the Rh1 deglycosylation (Figure 9D). In control experiments, the Rh1 MW did not change in *CG4784* null mutant (unpublished observations).

To confirm that phosphorylation of the residue $Ser^{73}$ inhibits α-Man-II activity, we generated transgenic flies expressing α-Man-II $^{S73G}$, a mutant variant with $Ser^{73}$ mutated to Gly (S73G). In *cn,dmppe,bw;GMR-Gal4/p[UAS::α-Man-II $^{S73G}$]* flies, the eye-specific expression of α-Man-II $^{S73G}$ successfully converted Rh1 to the extensively trimmed wild-type form in the *dmppe* mutant background (Figure 9E). In contrast, overexpression of a wild-type α-Man-II protein did not significantly affect Rh1 in the same genetic background. Thus, the dMPPE-dependent dephosphorylation of α-Man-II is critical for Rh1 deglycosylation (Figure 9F).

Once α-Man-II cleaves α1,3-linked and α1,6-linked mannoses from GnMan5Gn2, other glycosides will continue to remove the remaining GnMan3Gn2 from Rh1. We attempted to identify additional glycosides involved in Rh1 deglycosylation by generating mutants and/or RNAi knockdown flies for known and predicted glycosidase genes such as *edem1*, *edem2*, *png1*, *α-Man-I*, *α-Man-II b* and *CG14015*. In two *α-Man-II b* RNAi lines, we observed slightly increased MWs of Rh1 (Supplementary Figure S7). The potential role of *α-Man-IIb* in Rh1 deglycosylation will be further investigated in the future.

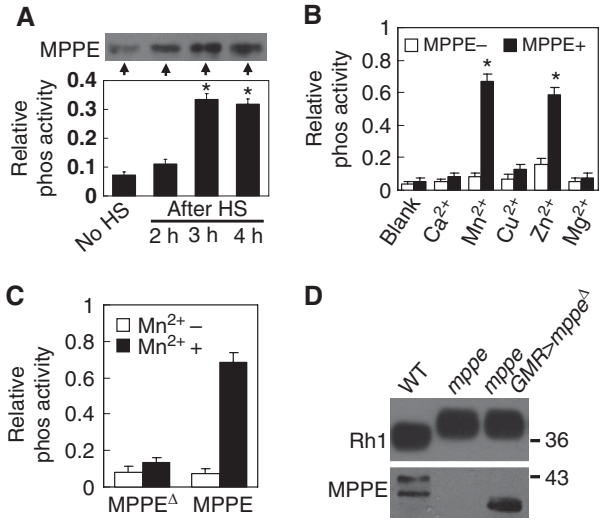


**Figure 7** dMPPE functions as a phosphoesterase. (**A**) Time courses of dMPPE expression (top, western blot) and phosphoesterase activity in fly head extracts (bottom). After heat shock at 37°C for 1 h, the heads of *p[hs::mppe]* transgenic flies were collected at different time points. The protein levels of dMPPE and total phosphoesterase activity of hydrolysed p-nitrophenyl phosphate were measured. The mean values and s.e.m. of three sets of data are presented. (**B**) Bacterially expressed dMPPE protein displays metal-dependent phosphoesterase activity. His-tagged dMPPE protein was expressed in *E. coli* and purified from cell lysate using an $Ni^{2+}$ affinity column. The phosphoesterase activity was measured by hydrolysis of p-nitrophenyl phosphate (pNpp). After averaging three sets of data, the mean values of phosphoesterase activity and s.e.m. are presented. (**C**) Phosphoesterase activity was abolished in truncated $dMPPE^{\Delta}$ protein, which deleted amino acid 164–183. After averaging three sets of data, the mean of phosphoesterase activity and s.e.m. are presented. (**D**) The phosphoesterase activity of dMPPE is essential for Rh1 deglycosylation. Eye-specific expression of truncated $dMPPE^{\Delta}$ cannot restore the MW of Rh1. dMPPE protein and truncated $dMPPE^{\Delta}$ protein levels are shown. *indicates that the sample is significantly different from the control ($P<0.01$; Student's *t*-test).

## Discussion

Our study has revealed that the deglycosylation of Rh1 rhodopsin is essential for its rapid transportation and stability, but is not required for its rhabdomeral targeting and signalling function. Most importantly, we have demonstrated that a phosphoesterase dMPPE mediates the process of Rh1 deglycosylation by dephosphorylating the glycosidase α-Man-II.

### *The role of dMPPE in the deglycosylation of rhodopsin*

Consistent with a previous microarray study (Xu *et al*, 2004), we demonstrated dMPPE to be predominately expressed in the retina, suggesting it might have an important role in the eye. Our work provides solid evidence that dMPPE is required for the oligosaccharide trimming in Rh1. To our knowledge, this is the first *in vivo* function identified for an MPPE.

The newly synthesized Rh1 protein in the ER contains a large oligosaccharide chain and has an MW of 40 kDa (Ozaki *et al*, 1993). In our experiments, nascent Rh1 rhodopsin existed as a 40-kDa protein, and it gradually changed to 39 kDa and remained the same size through eclosion in the *dmppe* mutant. These observations suggest that dMPPE is not critical for the initiation of deglycosylation in the ER. The 1-kDa shift in MW could be due to the cleavage of several saccharide residues in the ER, as it has been reported that ER glycosidases can remove three terminal glucose residues and some mannose residues from core oligosaccharide chains of glycoproteins (Helenius, 1994; Satoh *et al*, 1997). After transport to Golgi bodies, post-Golgi vesicles, and finally to rhabdomeral microvilli, the oligosaccharide chain is further processed to form a 36-kDa mature rhodopsin (Satoh *et al*, 1997). However, later steps of oligosaccharide trimming in Rh1, which occur in Golgi bodies and/or post-Golgi vesicles, require the activity of dMPPE.

dMPPE does not directly deglycosylate Rh1 as a glycosidase. Instead, it acts as a phosphoesterase, and promotes Rh1 deglycosylation through dephosphorylating α-Man-II. This is supported by our observations that the *α-Man-II* mutant had the same defect of Rh1 deglycosylation as the *dmppe* mutant, and that the defect in the *dmppe* mutant was rescued by a mutant variant of α-Man-II lacking the phosphorylation site.

In our study, a C-terminal His6-tagged dMPPE protein showed metal-dependent phosphoesterase activities in the presence of $Mn^{2+}$ or $Zn^{2+}$. This result is different from a previous work on PGAP5, the human MPPE. Although the activity of PGAP5 also depends on $Mn^{2+}$ and $Zn^{2+}$ (Fujita *et al*, 2009), an N-terminal His6-Flag-tagged PGAP5 did not recognize artificial phosphoesterase substrates p-nitrophenyl phosphate and monofluorophosphate. Instead, PGAP5 is reported as the enzyme that removes EtNP from the Man2 of GPI (Fujita *et al*, 2009). The lack of phosphoesterase activity in the N-terminal tagged PGAP5 could represent a difference between species. Alternatively, the N-terminal tag may have interfered with the recognition of substrates. Indeed, we also failed to detect any phosphoesterase activity in a purified N-terminal GST-tagged dMPPE protein (unpublished observations).

### *Phosphorylation regulates the α-Man-II activity*

We have identified a phosphorylation site in the fly α-Man-II at Ser-73, a residue conserved between mammals and *Drosophila* and residing in the lumen of ER (van den Elsen *et al*, 2001). It is previously reported that α-Man-II in mammalian HeLa and 3T3 cells also undergoes serine phosphorylation during post-translational modification (Moremen and Touster, 1985). Thus, the activity of mammalian α-Man-II is likely controlled in a similar manner through serine phosphorylation.

The functions of many proteins are regulated by phosphorylation/dephosphorylation in ER or Golgi. For example, phosphorylation/dephosphorylation serves as a sorting signal to determine the ER retention or Golgi transport for some proteins (Teh *et al*, 2009; Yellaturu *et al*, 2009). Phosphorylation/dephosphorylation modification also contributes to the control of enzymatic activity or the regulation of protein half-life (Hunter, 2007). Here, we have shown that the dephosphorylation of α-Man-II is required for its function in deglycosylation. This may provide the first evidence that the glycosylation status of membrane proteins can be regulated by phosphorylation in their secretory pathways.

### *The importance of Rh1 deglycosylation*

In vertebrates and some invertebrates, rhodopsin remains glycosylated after maturation (Hargrave, 1977; O'Tousa,

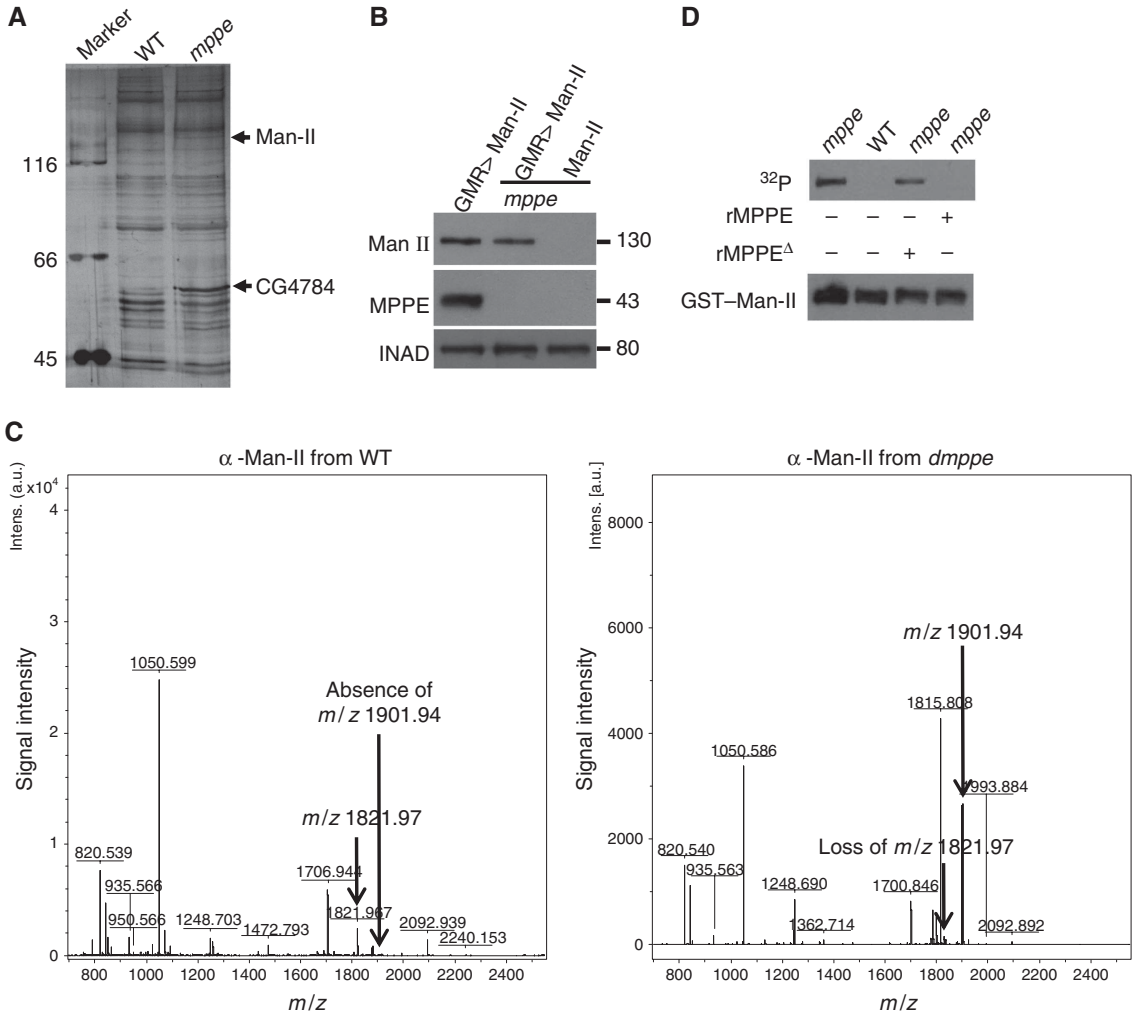


**Figure 8** dMPPE directly dephosphorylates α-Man-II. (**A**) Identification of phosphorylated proteins in *dmppe* mutants. Phosphorylated protein enrichment was performed as described in Materials and methods. Bands whose amount increased in the *dmppe* mutant sample were cut and identified by MS. Detailed results from the MS analysis are provided in Supplementary data. (**B**) Ectopic expression of α-Man-II in wild-type and *dmppe* mutant flies. (**C**) Identification of the phosphorylated peptide from the *dmppe* mutant. Myc-tagged α-Man-II was immunoprecipitated from wild-type and mutant flies. Trypsin-digested peptides were used for MS analysis. In the *dmppe* mutant sample, the *m/z* 1821.97 ion is lost with the appearance of an *m/z* 1901.94 ion. (**D**) dMPPE directly dephosphorylates α-Man-II *in vitro*. Phosphorylation and dephosphorylation reactions were performed as described in Materials and methods. Upper panel: Autoradiogram of SDS–PAGE of $^{32}$P *in vitro* labelled GST-α-Man-II recombinant protein. Lower panel: The same gel blotted and probed with antibodies to GST. rMPPE represents purified recombinant dMPPE and rMPPE$^{\Delta}$ represents purified recombinant truncated dMPPE.

1992; Brown *et al*, 1994). Intriguingly, the oligosaccharide of *Drosophila* Rh1 undergoes extensively trimming before maturation. The functional roles of oligosaccharide trimming in rhodopsin were not characterized, mostly due to the lack of a mutant that contains glycosylated rhodopsin in the rhabdomere. Although in several mutants, such as *ninaA*, Rh1 remains almost fully glycosylated, it is misfolded and accumulates in the ER (Colley *et al*, 1991). Rh1 accumulation in the ER triggers an ER stress, which in turn activates the unfolded protein response (Mendes *et al*, 2009). In contrast, in *dmppe* mutant, glycosylated Rh1 has no problem exiting the ER, which makes it a good model of study.

Using the *dmppe* mutant, we showed that the deglycosylation of rhodopsin is essential for the rapid transport of newly synthesized rhodopsin to rhabdomere. We further revealed that the retained oligosaccharide chain did not affect Rh1 localization and visual signalling. However, it does render Rh1 more sensitive to endocytic degradation, and leads to morphological and functional defects in the photoreceptor cells of aged *dmppe* mutant flies.

It has been proposed that N-glycans function as putative sorting signals (Fiedler and Simons, 1995; Gut *et al*, 1998). However, studies on the role of N-glycosylation in targeting membrane receptors to the cell surface showed variations among different receptors (Rands *et al*, 1990; Davis *et al*, 1995). Our study on Rh1 now suggests that N-glycosylation of rhodopsin is not required for its rhabdomeral localization. One explanation is that rhodopsin contains other intrinsic sorting signals that are sufficient to ensure its rhabdomeral targeting. Similarly, N-glycosylation was not necessary for the membrane targeting of several other membrane proteins (Chmelar and Nathanson, 2006).

One potential role of N-glycosylation is to make the protein more stable and more resistant to proteolysis (Kundra and Kornfeld, 1999). Surprisingly, our results showed that the glycosylated Rh1 was not as stable as the extensive trimmed

 

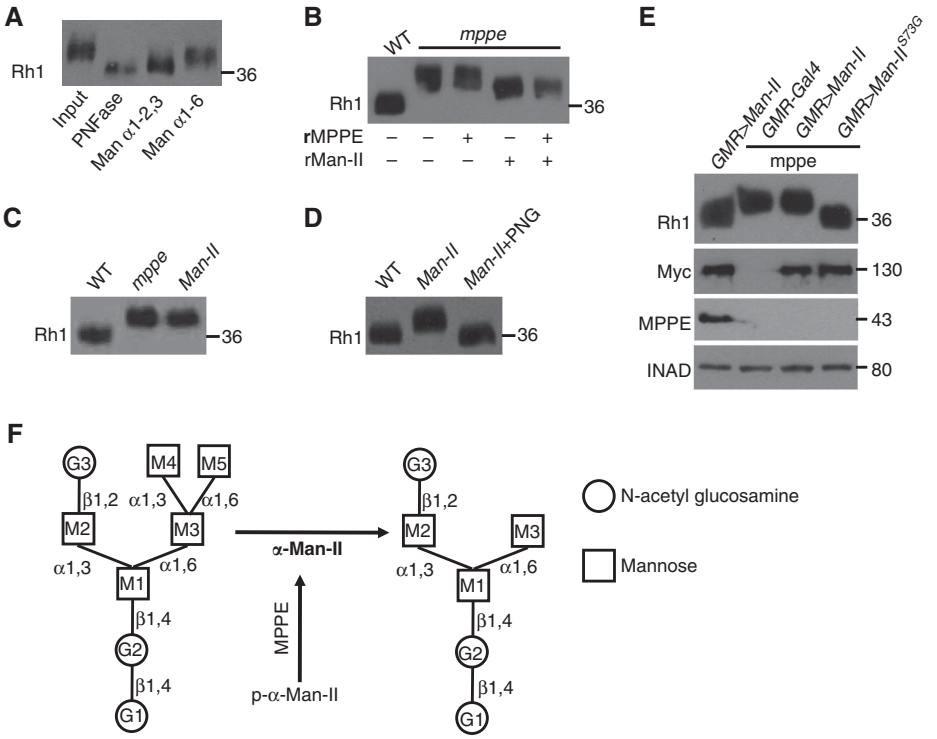


**Figure 9** α-Man-II mediates Rh1 deglycosylation *in vivo*. (**A**) The MW of Rh1 was reduced after treatment with α1-6 mannosidase or α1-2,3 mannosidase. Purified Rh1 was incubated with different glycosidases at 37°C for 16 h. (**B**) The MW of Rh1 was reduced after digestion with recombinant α-Man-II. Recombinant dMPPE and GST-α-Man-II were purified as described in Materials and methods. Purified Rh1 was incubated with GST–α-Man-II alone or with the mixture of GST–α-Man-II and dMPPE in 37°C for 16 h. rMPPE represents purified recombinant dMPPE and rMan-II represents purified recombinant GST–α-Man-II. Note that the activity of recombinant α-Man-II does not depend on the presence of dMPPE. (**C**) The MW of Rh1 from the *α-Man-II* mutant was similar to that of the *dmppe* mutant. (**D**) The MW of Rh1 from *α-Man-II* mutant was reduced after digestion with PNGase F. (**E**) Expression of the mutant form α-Man-II$^{S73G}$, but not wild-type α-Man-II, restored the MW of Rh1 in the *dmppe* mutant background. α-Man-II (Myc) and dMPPE expression levels are shown. (**F**) The role of dMPPE in Rh1 deglycosylation. dMPPE directly dephosphorylates α-Man-II, which in turn removes two mannoses from the oligosaccharide chain of Rh1. N-acetylglucosamine residues are shown as circles and mannose residues are shown as squares.

form after being internalized through light-stimulated endocytosis. Considering that the glycosylated Rh1 does not contain a complete core oligosaccharide chain and could have exposed oligomannose, one explanation for its reduced stability is that the oligomannose may promote entry of the endocytic Rh1 protein into lysosomes for degradation. This effect of oligomannoside has been demonstrated for both membrane glycoproteins (Ward *et al*, 1995; Wiertz *et al*, 1996) and soluble glycoproteins (Qu *et al*, 1996).

## Materials and methods

### *Fly genetics*

P-element insertion line *pBacCG8889*$^{e02905}$ was obtained from the Exelixis Collection at Harvard Medical School. To exclude the effect of pigments, all wild-type and *pBacCG8889*$^{e02905}$ mutant flies in this work had a *cn,bw* background. The dark-reared flies were never exposed to light from the early pupal stage; all other flies were raised in an approximate 12 h light (700 lux)/12 h dark cycle. Other fly genetics information was supplied in Supplementary data.

### *Antibodies*

The dMPPE antibody was raised in rabbits against synthesized peptide (aa 341–355) of dMPPE protein and generated by Signalway Antibody Co. Let. (Nanjing, China). An affinity column, which was created by coupling full-length dMPPE to Sepharose 4B, was used to purify the antibody. The sources of other antibodies were DSHB (Rh1), C Zuker (Rh1 polyclone antibodies), C Montell (INAD) and Abcam (Myc-tag).

### *Glycosidases*

Peptide: N-Glycosidase F (PNGase F), Endoglycosidase H, α1-6 mannosidase and α1-2,3 mannosidase were purchased from New England Biolabs Inc. α1-6 mannosidase specifically removes unbranched α1-6 linked D-mannopyranosyl residues from oligosaccharides, whereas α1-2,3 mannosidase specifically catalyses the hydrolysis of α1-2 and α1-3 linked D-mannopyranosyl residues from oligosaccharides.

### *Electrophysiological recordings and relative light sensitivity recording*

ERGs were recorded as previously described (Han *et al*, 2006). The signal was amplified and recorded using a Warner IE210 Intracellular Electrometer.

For relative light sensitivity measuring, orange light pulses of increasing intensities were used to stimulate responses in the eye. Before recording, the flies were allowed to adapt for 5 min in the dark. The relative light sensitivity of a photoreceptor is defined as $I/I_{WT}$, where $I_{WT}$ represents the mean light intensity of triggering a detectable response in the wild-type eye, and $I$ is the lowest light intensity for the individual eye examined. For each genotype and condition, 12 flies were examined and the relative sensitivities were averaged to obtain a mean. The standard error of the mean (s.e.m.) was calculated and presented as error bar in the figures.

### *Immunostaining and quantitative analysis*

For immunofluorescence staining, fly heads were fixed with 4% paraformaldehyde in PBS, dehydrated with acetone and embedded in LR White resin. For dark-reared flies, fly heads were bisected in $<5$ min with dim red light, and fixation was performed in complete dark. One-micrometer sections were cut across the top half of the eye. A monoclonal Rh1 antibody (DSHB) and FITC-conjugated

secondary antibodies were used for Rh1 labelling, TRITC-conjugated phalloidin were used for F-actin staining. The stained sections were examined under a ZEISS Axio observer A1 microscope.

For quantitative analyses of the ratio of Rh1 load in the rhabdomeres in Figure 3C and D, fluorescence images obtained were analysed with ImageJ software (National Institute of Health, USA). The ratio of Rh1 present in the rhabdomeres (R) was calculated using the formula $R = (Ir-Ib)/((Ir-Ib) + (Ic-Ib))$, where *Ir*, *Ib* and *Ic* are the fluorescence intensities in the rhabdomeres, in the background, and in the cell body, respectively. Background intensities were determined in the centre of the ommatidium where the rhabdomere of the R7/R8 cells does not contain Rh1.

For quantitative analyses of the ratio of endocytosed Rh1 signal in Figure 4E, fluorescence images obtained were analysed with ImageJ software (National Institute of Health, USA). The total fluorescence intensities (*It*) were adjusted according to the quantification of total Rh1 protein level in Figure 4F. $It = ((Ir-Ib) + (Ic-Ib))$, where *Ir*, *Ib* and *Ic* are the fluorescence intensities in the rhabdomeres, in the background, and in the cell body, respectively. Background intensities were determined in the centre of the ommatidium where the rhabdomere of the R7/R8 cells does not contain Rh1. Then, the ratio of endocytosed Rh1 signal (*R*) was calculated using the formula $R = (Ic-Ib)/Ito$, where *Ito* represents the adjusted total fluorescence intensities in dark-reared flies.

For dMPPE labelling, ommatidia were dissected in ringer solution without calcium, transferred to the Poly-L-Lysine coated slides and kept in dark for 30 min. Sections were fixed and costained with Rh1 antibody (1:100) and dMPPE antibody (1:50). The stained samples were examined under an LSM 510 confocal microscope.

### Histological fixation, sectioning and EM

Histological analysis was performed as follows: fly heads were bisected and fixed at 4°C for 12 h in 2.5% gluteraldehyde, 0.1 M sodium cacodylate (pH 7.2). After rinse with 0.1 M sodium cacodylate for three times, the fixed tissue was stained with 1% osmium tetroxide for 1 h at room temperature. A standard ethanol dehydration series was performed and the tissue was immersed in two 10 min washes of propylene oxide. The tissue was then embedded with standard procedures. For EM, thin sections (100 nm) were cut, collected on Cu support grids, and stained with uranyl acetate for 8 min, followed by 5 min with lead citrate. Micrographs were taken at 80 KV on Hitachi-7650.

To examine the localization of Rh1 with electron microscope (EM), fly heads were bisected in $<5$ min with dim red light, and fixation was performed in complete dark. Fixed fly heads were embedded in LR White as described (Li and Montell, 2000), except that ethanol was used for the dehydration. Thin sections (100 nm) were cut and immunostained with the primary antibodies and then with an anti-mouse IgGs conjugated with gold particles. The particle sizes are 15 nm for the Rh1 labelling. After staining with 1% aqueous uranyl acetate, the sections were examined using a transmission EM.

### Rh1 affinity chromatography

To purify Rh1 from wild-type and the *dmppe* mutants, an affinity column was created by coupling Rh1 antibody (4C5) to Sepharose 4B (Amersham-Pharmacia, Inc.). In all, 2000 heads were collected and homogenized in sodium phosphate buffer containing 1% CHAPS. Supernatant was loaded onto affinity column after centrifugation at 150 000 *g* for 60 min. After rinsing, Rh1 and its associated proteins were eluted with 100 mM glycine. The eluted samples were dialysed and concentrated.

### Phosphorylated protein enrichment and in vitro phosphorylation assays

In all, 3000 heads were collected from 1-day-old wild-type flies and *dmppe* mutants, respectively. Heads were homogenized in sodium phosphate buffer containing 1% CHAPS and 1% Triton X-100. Phosphorylated proteins were enriched by TALON PMAC phosphoprotein enrichment kit (Clontech) according to the user manual. The equal eluted samples were subjected to SDS–PAGE and silver stained.

*In vitro* phosphorylation assays were performed as described (Alloway and Dolph, 1999). Briefly, 10 fly heads ($<2$ days) were dissected and homogenized in 20 µl assay buffer (16 mM Tris, pH 7.5, 5 mM $MgCl_2$, 5 mM β-mercaptoethanol, 2 mM $MnCl_2$). Phosphorylation reactions were performed in room temperature for 15 min in 15 µl assay buffer with 0.02 µg purified recombinant GST-α-Man-II, 0.3 µCi [$\gamma$-$^{32}$P]ATP (3000 Ci/mmol), and 3 µl of homogenate. For dephosphorylation reactions, 0.01 µg purified recombinant dMPPE or truncated dMPPE$^{\Delta}$ was added for further 15 min incubation. The GST–α-Man-II was precipitated by glutathione-Sepharose beads (Amersham Biosciences) and subjected to SDS–PAGE, autoradiography and western analysis with antibodies against GST.

### Identification of phosphorylation site in α-Man-II by MS

Myc-tagged α-Man-II was immunoprecipitated from wild-type and mutant flies by using EZview red anti-c-myc Affinity gel (Sigma). Gel bands were excised, destained and digested with proteomics grade trypsin (Sigma) at 37°C for 18 h. Peptides were desalted using a ZipTip (C18; Millipore) and spotted for mass spectrometric analysis on an MALDI-TOF/TOF analyzer. Phosphorylated peptides of α-Man-II were isolated from trypsin-digested sample by using PHOS-select iron affinity gel (Sigma). Amino-acid sequences were identified by subjecting peptides to collision-induced dissociation during MALDI-TOF-MS/MS.

### Statistics

For each quantitative analysis, three sections from three flies were examined in Figures 1, 3, 4, 5, with $>30$ ommatidia counted in each section. After averaging three sets of data, the mean values and s.e.m. (as error bar) were presented.

### Supplementary data

Supplementary data are available at *The EMBO Journal* Online (http://www.embojournal.org).

## Acknowledgements

We thank Charles S Zuker for *ninaE*$^{17}$,*p[ninaE*::*ninaE*$^{\Delta 356}$*]* flies and polyclone anti-Rh1 antibody; Craig Montell for anti-INAD antibody; Bloomington Stock Center, Kyoto Drosophila Stock Center, Harvard Exelixis Collection and Vienna Drosophila RNAi Center for the flies; Fuqiang Wang for the MS analysis; Ming Fang, Liudi Yuan and people in the Han laboratory for critical comments on the manuscript. This work was supported by National Natural Science Foundation of China (30970663 and 31070683) and New-Century Training Program Foundation for the Talents by the State Education Commission and Youth Foundation of southeast university to JH; NIH grant R01-AG022508 and R01-EY019060 to HL; National Natural Science Foundation of China (Key program 30930051) to WX.

*Author contributions*: JC, JH and HL conceived and designed the experiments. JC, YL, KR, WJX and WH performed the experiments. YL and JH analysed the data. WX contributed reagents and oversaw the research. JH, HL and KR wrote the paper.

## Conflict of interest

The authors declare that they have no conflict of interest.

## References

Alloway PG, Dolph PJ (1999) A role for the light-dependent phosphorylation of visual arrestin. *Proc Natl Acad Sci USA* **96:** 6072–6077

Aravind L, Koonin EV (1998) Phosphoesterase domains associated with DNA polymerases of diverse origins. *Nucleic Acids Res* **26:** 3746–3752

 

Brown G, Chen DM, Christianson JS, Lee R, Stark WS (1994) Receptor demise from alteration of glycosylation site in Drosophila opsin: electrophysiology, microspectrophotometry, and electron microscopy. *Vis Neurosci* **11:** 619–628

Chen S, Yakunin AF, Kuznetsova E, Busso D, Pufan R, Proudfoot M, Kim R, Kim SH (2004) Structural and functional characterization of a novel phosphodiesterase from Methanococcus jannaschii. *J Biol Chem* **279:** 31854–31862

Chmelar RS, Nathanson NM (2006) Identification of a novel apical sorting motif and mechanism of targeting of the M2 muscarinic acetylcholine receptor. *J Biol Chem* **281:** 35381–35396

Cohen P (1989) The structure and regulation of protein phosphatases. *Annu Rev Biochem* **58:** 453–508

Colley NJ, Baker EK, Stamnes MA, Zuker CS (1991) The cyclophilin homolog ninaA is required in the secretory pathway. *Cell* **67:** 255–263

Davis D, Liu X, Segaloff DL (1995) Identification of the sites of N-linked glycosylation on the follicle-stimulating hormone (FSH) receptor and assessment of their role in FSH receptor function. *Mol Endocrinol (Baltimore, MD)* **9:** 159–170

Dryja TP, Li T (1995) Molecular genetics of retinitis pigmentosa. *Hum Mol Genet* **4:** 1739–1743

Dwek RA (1996) Glycobiology: toward understanding the function of sugars. *Chem Rev* **96:** 683–720

Fiedler K, Simons K (1995) The role of N-glycans in the secretory pathway. *Cell* **81:** 309–312

Fliesler SJ, Rapp LM, Hollyfield JG (1984) Photoreceptor-specific degeneration caused by tunicamycin. *Nature* **311:** 575–577

Fliesler SJ, Rayborn ME, Hollyfield JG (1986) Inhibition of oligosaccharide processing and membrane morphogenesis in retinal rod photoreceptor cells. *Proc Natl Acad Sci USA* **83:** 6435–6439

Fujita M, Maeda Y, Ra M, Yamaguchi Y, Taguchi R, Kinoshita T (2009) GPI glycan remodeling by PGAP5 regulates transport of GPI-anchored proteins from the ER to the Golgi. *Cell* **139:** 352–365

Gut A, Kappeler F, Hyka N, Balda MS, Hauri HP, Matter K (1998) Carbohydrate-mediated Golgi to cell surface transport and apical targeting of membrane proteins. *EMBO J* **17:** 1919–1929

Han J, Gong P, Reddig K, Mitra M, Guo P, Li HS (2006) The fly CAMTA transcription factor potentiates deactivation of rhodopsin, a G protein-coupled light receptor. *Cell* **127:** 847–858

Han J, Reddig K, Li HS (2007) Prolonged G(q) activity triggers fly rhodopsin endocytosis and degradation, and reduces photoreceptor sensitivity. *EMBO J* **26:** 4966–4973

Hargrave PA (1977) The amino-terminal tryptic peptide of bovine rhodopsin. A glycopeptide containing two sites of oligosaccharide attachment. *Biochim Biophys Acta* **492:** 83–94

Harpaz N, Schachter H (1980) Control of glycoprotein synthesis. Processing of asparagine-linked oligosaccharides by one or more rat liver Golgi alpha-D-mannosidases dependent on the prior action of UDP-N-acetylglucosamine: alpha-D-mannoside beta 2-N-acetylglucosaminyltransferase I. *J Biol Chem* **255:** 4894–4902

Helenius A (1994) How N-linked oligosaccharides affect glycoprotein folding in the endoplasmic reticulum. *Mol Biol Cell* **5:** 253–265

Helenius A, Aebi M (2001) Intracellular functions of N-linked glycans. *Science (New York, NY)* **291:** 2364–2369

Hoffmeister KM, Josefsson EC, Isaac NA, Clausen H, Hartwig JH, Stossel TP (2003) Glycosylation restores survival of chilled blood platelets. *Science (New York, NY)* **301:** 1531–1534

Huber A, Smith DP, Zuker CS, Paulsen R (1990) Opsin of Calliphora peripheral photoreceptors R1-6. Homology with Drosophila Rh1 and posttranslational processing. *J Biol Chem* **265:** 17906–17910

Hunter T (2007) The age of crosstalk: phosphorylation, ubiquitination, and beyond. *Mol Cell* **28:** 730–738

Johnson EC, Pak WL (1986) Electrophysiological study of Drosophila rhodopsin mutants. *J Gen Physiol* **88:** 651–673

Katanosaka K, Tokunaga F, Kawamura S, Ozaki K (1998) N-linked glycosylation of Drosophila rhodopsin occurs exclusively in the amino-terminal domain and functions in rhodopsin maturation. *FEBS Lett* **424:** 149–154

Keppetipola N, Shuman S (2008) A phosphate-binding histidine of binuclear metallophosphodiesterase enzymes is a determinant of 2′,3′-cyclic nucleotide phosphodiesterase activity. *J Biol Chem* **283:** 30942–30949

Kornfeld R, Kornfeld S (1985) Assembly of asparagine-linked oligosaccharides. *Annu Rev Biochem* **54:** 631–664

Kundra R, Kornfeld S (1999) Asparagine-linked oligosaccharides protect Lamp-1 and Lamp-2 from intracellular proteolysis. *J Biol Chem* **274:** 31039–31046

Leonard DS, Bowman VD, Ready DF, Pak WL (1992) Degeneration of photoreceptors in rhodopsin mutants of Drosophila. *J Neurobiol* **23:** 605–626

Li HS, Montell C (2000) TRP and the PDZ protein, INAD, form the core complex required for retention of the signalplex in Drosophila photoreceptor cells. *J Cell Biol* **150:** 1411–1422

Mendes CS, Levet C, Chatelain G, Dourlen P, Fouillet A, Dichtel-Danjoy ML, Gambis A, Ryoo HD, Steller H, Mollereau B (2009) ER stress protects from retinal degeneration. *EMBO J* **28:** 1296–1307

Moremen KW, Touster O (1985) Biosynthesis and modification of Golgi mannosidase II in HeLa and 3T3 cells. *J Biol Chem* **260:** 6654–6662

O'Tousa JE (1992) Requirement of N-linked glycosylation site in Drosophila rhodopsin. *Vis Neurosci* **8:** 385–390

Ozaki K, Nagatani H, Ozaki M, Tokunaga F (1993) Maturation of major Drosophila rhodopsin, ninaE, requires chromophore 3-hydroxyretinal. *Neuron* **10:** 1113–1119

Papermaster DS (1995) Necessary but insufficient. *Nat Med* **1:** 874–875

Partridge EA, Le Roy C, Di Guglielmo GM, Pawling J, Cheung P, Granovsky M, Nabi IR, Wrana JL, Dennis JW (2004) Regulation of cytokine receptors by Golgi N-glycan processing and endocytosis. *Science (New York, NY)* **306:** 120–124

Qu D, Teckman JH, Omura S, Perlmutter DH (1996) Degradation of a mutant secretory protein, alpha1-antitrypsin Z, in the endoplasmic reticulum requires proteasome activity. *J Biol Chem* **271:** 22791–22795

Rands E, Candelore MR, Cheung AH, Hill WS, Strader CD, Dixon RA (1990) Mutational analysis of beta-adrenergic receptor glycosylation. *J Biol Chem* **265:** 10759–10764

Rudd PM, Elliott T, Cresswell P, Wilson IA, Dwek RA (2001) Glycosylation and the immune system. *Science (New York, NY)* **291:** 2370–2376

Satoh A, Tokunaga F, Kawamura S, Ozaki K (1997) *In situ* inhibition of vesicle transport and protein processing in the dominant negative Rab1 mutant of Drosophila. *J Cell Sci* **110** (Part 23)**:** 2943–2953

Satoh AK, O'Tousa JE, Ozaki K, Ready DF (2005) Rab11 mediates post-Golgi trafficking of rhodopsin to the photosensitive apical membrane of Drosophila photoreceptors. *Development (Cambridge, England)* **132:** 1487–1497

Teh EM, Chai CC, Yeong FM (2009) Retention of Chs2p in the ER requires N-terminal CDK1-phosphorylation sites. *Cell Cycle* **8:** 2964–2974

Twining SS (1984) Fluorescein isothiocyanate-labeled casein assay for proteolytic enzymes. *Anal Biochem* **143:** 30–34

van den Elsen JM, Kuntz DA, Rose DR (2001) Structure of Golgi alpha-mannosidase II: a target for inhibition of growth and metastasis of cancer cells. *EMBO J* **20:** 3008–3017

Varki A (1993) Biological roles of oligosaccharides: all of the theories are correct. *Glycobiology* **3:** 97–130

Vinos J, Jalink K, Hardy RW, Britt SG, Zuker CS (1997) A G protein-coupled receptor phosphatase required for rhodopsin function. *Science (New York, NY)* **277:** 687–690

Ward CL, Omura S, Kopito RR (1995) Degradation of CFTR by the ubiquitin-proteasome pathway. *Cell* **83:** 121–127

Webel R, Menon I, O'Tousa JE, Colley NJ (2000) Role of asparagine-linked oligosaccharides in rhodopsin maturation and association with its molecular chaperone, NinaA. *J Biol Chem* **275:** 24752–24759

Wiertz EJ, Jones TR, Sun L, Bogyo M, Geuze HJ, Ploegh HL (1996) The human cytomegalovirus US11 gene product dislocates MHC class I heavy chains from the endoplasmic reticulum to the cytosol. *Cell* **84:** 769–779

Xu H, Lee SJ, Suzuki E, Dugan KD, Stoddard A, Li HS, Chodosh LA, Montell C (2004) A lysosomal tetraspanin associated with retinal degeneration identified via a genome-wide screen. *EMBO J* **23:** 811–822

Yellaturu CR, Deng X, Cagen LM, Wilcox HG, Mansbach II CM, Siddiqi SA, Park EA, Raghow R, Elam MB (2009) Insulin enhances post-translational processing of nascent SREBP-1c by promoting its phosphorylation and association with COPII vesicles. *J Biol Chem* **284:** 7518–7532